Cryst. Res. Technol.	37	2002	9	983–1010

V. I. TALANIN*, I. E. TALANIN, D. I. LEVINSON

Zaporozhye State Engineering Academy, Lenin avenue 226, 69006 Zaporozhye, Ukraine

Physical Model of Paths of Microdefects Nucleation in Dislocation-Free Single Crystals Float-Zone Silicon

With the help of selective etching, transmission electron microscopy complex researches of non-doped dislocation-free single crystals of float-zone silicon by a diameter of 30 mm were conducted. The crystals were obtained with various growth rates and were subjected to various kinds of technological effects. Is established that the process of microdefects formation in silicon proceeds simultaneously on two independent mechanisms: vacancy and interstitial. The physical model of formation of microdefects in dislocation-free monocrystals of FZ silicon is offered.

Keywords: silicon, point defects, self-interstitials, vacancies, microdefects

(Received August 15, 2001; Accepted July 8, 2002)

1.Introduction

It is well known that the formation of structural microdefects in dislocation-free single crystals of silicon is stipulated by temperature conditions of crystal growth [1-3]. Structural microdefects formed during cooling of crystals after their growth which may include agglomerates of point defects (vacancies or silicon self-interstitial) and impurities. Since only high purity silicon can be used in modern electronic industry knowledge of processes of formation of defects in a semiconducting material is necessary [4, 5].

The systematic study of microdefects began since 1960's, using methods of selective etching, decoration and X-ray topography [6-9]. Two types of microdefects were identified: A-microdefects (usually revealed as large etch-pits with smaller concentration) and B-microdefects (small etch-pits with higher concentration) [1, 10, 11]. With the help of transmission electron microscopy (TEM) it was established that A-microdefects [12] and B-microdefects [13, 14] have an interstitial nature. The A-microdefects are observed in stratified distribution at a crystal growth rates of V = 1…3.5 mm/min, and in uniform distribution at V < 1 mm/min. B-microdefects are observed in stratified distribution at V ≤ 4.5 mm/min. Stratified distribution of microdefects showed the distribution of their nucleation sites. During growth of crystal the fluctuations of temperatures due by rotation of crystal and a convection of a melt take place [15]. Therefore, the microdefects grow, repeating growth of crystal and stop of growth [15, 16].

The further studies of monocrystals of silicon grown at high growth rates (more than 5 mm/min) have shown that these monocrystals contain uniformly distributed microdefects. This was revealed by selective etching as matt areas. The authors, who observed these defects [2] by selective etching and decoration techniques classified them as C- and D-

* corresponding author: rio@zgia.zp.ua

© 2002 WILEY-VCH Verlag GmbH & Co. KGaA, Weinheim 0232-1300/02/0909-0983 $ 17.50+.50/0

microdefects depending on their distribution. Both of these types of microdefects were found as areas of uniformly distributed defects with high densities. The difference between C- and D-defects was in distribution of microdefects in these areas. D-microdefects are usually concentrated as channels in a central part of crystal whereas C-microdefects are revealed as rings or contours of the incorrect form. Roksnoer et al. [17], using a X-ray topography followed by decoration with copper suggested that D-microdefects have a vacancy character. Using TEM the authors of Refs. [14, 18-20] investigated in detail the nature of D-microdefects, which were found in Ref. [2]. It was established that D-microdefects (as well as C-microdefects) formed in the crystals which were obtained at growth rates more than 4.5 mm/min, have an interstitial nature. Furthermore, in the areas where uniformly distributed D-defects were not revealed by selective etching, vacancy microdefects which coexist together with interstitials microdefects were detected with TEM [18, 19]. This results are confirmed in the recent report of Bublik et al. [21]. They revealed microdefects in silicon by X-rays diffuse scattering. These authors obtained results about defects which will be formed in "interstitial" and "vacancy" regimes of growth (which were interpreted as A-, B- and A'-defects). These results allowed the authors to make a conclusion that all these defects are interstitial type. Furthermore, they detected other defects which have other sign of a strain, i.e. defects a vacancy type in the same areas of crystal where the interstitials defects were observed. The results of Ref. [21] as well as results of Refs. [14, 18-20] also are confirmed by other recent researches [22-26]. Many of these Refs. is discuss Czochralski-grown silicon. Therefore, it is possible to think that the processes of defect formation in both of these types of crystals are identical [27].

Thus, the results [17] cannot be represented as "incorrect". Since vacancy microdefects and interstitials microdefects coexist, the vacancy microdefects detected in [17] are not D-microdefects according to the classification [2]. The difference between the classifications [2] and [17] are not basic, but they can cause disagreement in the determination of the types of microdefects. In this paper we shall use the classification [2]. Furthermore, in Ref. [17] was studied CZ-Si, in which revealing of interstitial D-microdefects is very difficult in a comparison with FZ-Si [14].

Summarizing all experimental results about a physical nature of microdefects in dislocation-free single crystals FZ-Si with the diameter of 30 mm, then according to a classification [2] it is possible to conclude that A-microdefects are interstitial dislocation loops with the sizes of 1...50 μm with a Burgers vector of $\overline{b} = 1/2$ [110], which are in planes {111} and {110}. B-microdefects are agglomerates of point defects of an interstitial type with sizes of 20...50 nm which are in planes {100} and {111}. D-microdefects of an interstitial type are agglomerates of point defects with the sizes of 4…10 nm. C-microdefects completely are identical D-microdefects on TEM-images, sign of a strain crystalline lattice and sizes. Therefore to select them as a other type of microdefects is inexpedient. Was suggested [18] that D-microdefects are uniformly distributed B-microdefects. Was established what in crystals which were obtained at high growth rates (more than 6 mm/min) microdefects of vacancy type are formed simultaneously with microdefects of interstitial type in the same regions of crystal.

Various theoretical models were suggested to explain the regularities of formation of microdefects in silicon. Main problems were the assumptions about the dominant type of point defects in crystal, their concentration, and interaction among themselves. In some models [12, 16, 28, 29] it was assumed that the dominating type of point defects in crystal

are are self-interstitials. In other models [15, 30-32] it was supposed that the dominating type of defects are the vacancies. In contrast, authors of Refs. [33, 34] suggested simultaneous independent coexistence of both main types of point defects at high temperatures. However none of these models could explain experimental results, which were obtained later with the help of TEM [35].

According to the commonly accepted Voronkov theory [36-38], the recombination rate between isolated vacancy and interstitial defects is high and further the diffusivity of interstitials is higher than the diffusivity of vacancies near the melting point and finally the concentrations of vacancies is higher than the concentrations of interstitials at the melting point, where both concentrations are in thermal equilibrium. Only the microdefects of either interstitial type (A- and B-microdefects, if the concentration of self-interstitials is higher than concentration of vacancies) or only a vacancy type (D-microdefects, if the concentration of vacancies is higher than concentration of interstitial atoms) are formed in the crystal. According to [36], the type of dominating point defects depends on the parameter V/G (V - growth rate of crystal, G - axial temperature gradient): if $V/G < C_{crit}$, then interstitial atoms of silicon dominate in the crystal, if $V/G > C_{crit}$, then the vacancies dominate. Furthermore, these results based on data from Refs. [16, 17].

Thus, the sense of a Voronkov model consists of the following: a) existence of recombination between self-interstitials and vacancies for temperatures close to temperature of smelting; b) was supposed that only vacancy nature for primary grown-in microdefects; c) independent existence areas with only interstitial and only vacancy microdefects.

However, these results, which are mainly theoretical conclusions which were not changed since 1982 [36], can not explain some latest experimental results [14, 18-27, 39, 40]. Furthermore, Voronkov's theory does not take into account the influence of carbon to process of formation of microdefects. The participation of carbon during defect formation results in a conclusion about a heterogeneous character of nucleation of microdefects [23, 26, 41]. Therefore, the purpose of our paper is the development of an optimum physical model of formation, growth and transformation of microdefects in FZ silicon.

2. Experimental Methods

Non-doped monocrystals of high resistivity (2200…4000 Ωcm) n-type silicon were grown by float zone technique in vacuum. The number of passes of a melting zone varied from 2 up to 10. The concentration of oxygen and carbon, defined by IR-absorption was less than $5 \cdot 10^{15}$ cm^{-3}. The crystals received at a constant growth rate in a range 1…9 mm/min. Some crystals were obtained with modification of growth rate on fixed length. Furthermore, in some cases the growth of the crystal was stopped for 30 or 60 min, and was resumed after that. To freeze-in the initial stages of formation of microdefects we conducted quenching of crystals. To study the reasons of formation of microdefects the crystals were subjected to special thermal processings. Furthermore, to confirm the influence of oxygen on formation of microdefects, the experiments with intentional doping of crystals by oxygen were conducted. The oxygen doping was carried out from a gas phase at adding the steams of H_2O_2 to the growth chamber.

The full study of processes of microdefects formation and transformation is very important. Therefore we deliberately used in our work crystals by a diameter of 30 mm. In such crystals if growth condition are changed we can observe all types of microdefects.

When the crystals diameter is increased the growth condition are changed. In result in large-scale crystals we can observe only some types of microdefects. Furthermore, the growth of large-scale crystals is limited by technology and equipping. In large-scale crystals the range of growth rates decreases on a comparison with a crystals of small diameters.

The method of selective etching of the cross-sections of crystal [42, 43] with subsequent TEM-analysis was used to reveal the distribution of grown-in microdefects. The TEM-studies were conducted by methods "black-white contrast" [see, e.g. 44-46], 2,5D [see, e.g. 47, 48] and "inside-outside contrast" [49]. Was applied electronic microscope JEM-7A and TSEM-200 with accelerating voltage up to 100 kV. For such voltage the introduction of radiation defects is excluded, i.e. the quality of experiment is improved.

3.Results

3.1. The process of transformation grown-in microdefects: influence of a high-temperature processing

During production of semiconducting devices the initial monocrystals of silicon are subjected to various thermal processings. In result of these processings the microdefects can be transformed [50, 51]. It is supposed [18], that D-microdefects are an initial stage of formation of interstitial defects, which then are transformed in B- and A-microdefects. Thus, it is important to determine how the process of transformation of the initial grown-in D-microdefects proceeds. The methods of our experiments in particularly is shown in Refs. [52, 53].

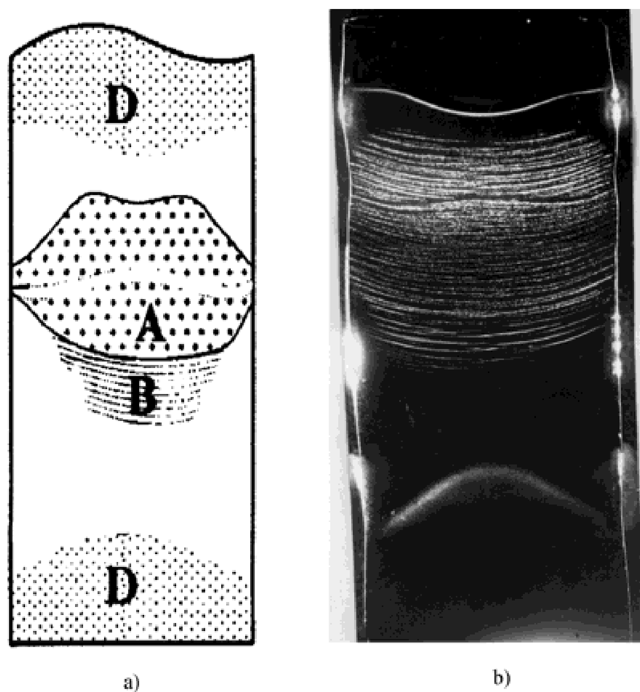

Fig. 1: Microdefects distribution at V = 6 mm/min after stop of growth (diameter 30 mm), (a)– schematic representation, (b) – selective etching.

The experiments on thermal processing were conducted in two stages. On the first stage (I) the crystals obtained at V = 6 mm/min with a stop of growth during 60 min were investigated using selective etching and TEM. The same crystals were cut in four parts, each of which then was cut in halves along {112} planes. One half of each of the cut ingots was subjected to selective etching to reveal microdefects. The other half was subjected to thermal processing in vacuum during 60 min at the temperature of 800, 900, 1000, 1100°C respectively. On the second stage (II) the crystals obtained at growth rates 2, 3, 6, 8 mm/min respectively were subjected to thermal processing (within 3 hours) at the temperature of 1100°C in hydrogen atmosphere.

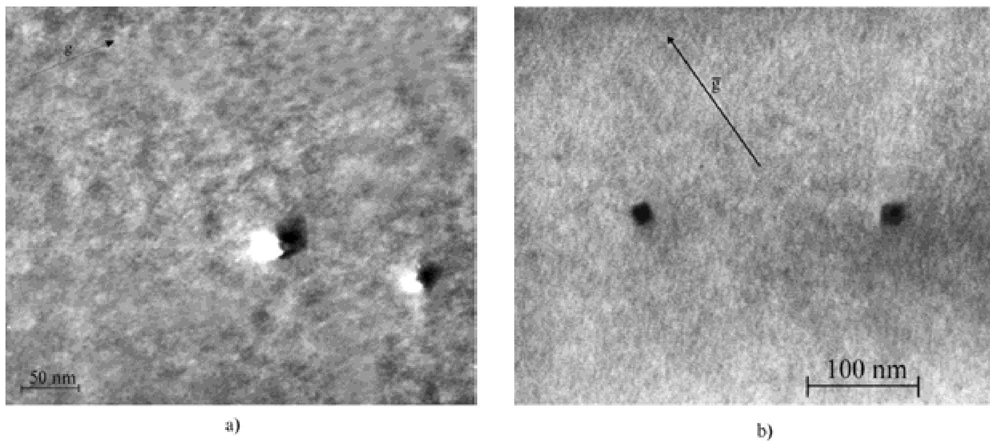

Fig. 2: B-microdefects after crystal thermal processing (V = 6 mm/min, after stop of growth), dark field, (a) - $\bar{g} = (\bar{2}20)$, (b) - $\bar{g} = (\bar{2}02)$.

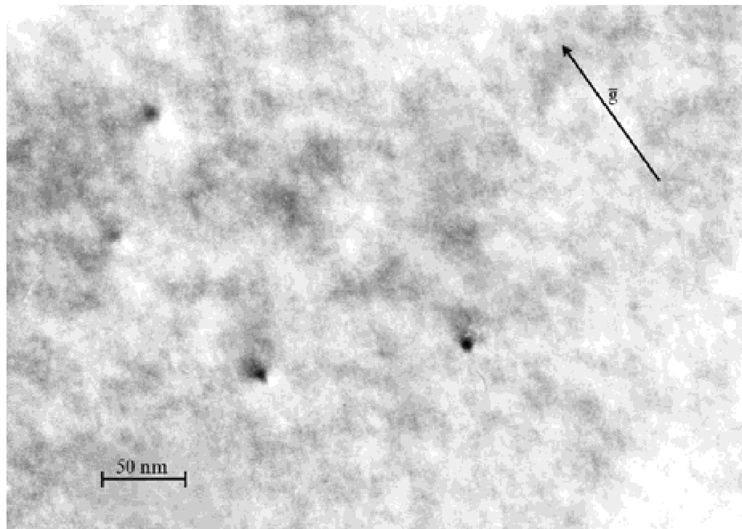

Fig. 3: D-microdefects after crystal thermal processing (V = 6 mm/min, after stop of growth), dark field, $\bar{g} = (2\bar{2}0)$.

I. The images of distribution of microdefects in crystal, which was obtained with a stop of growth, are shown in a Fig. 1. At the V = 6 mm/min only grown-in D-microdefects in uniform distribution are observed. As shown, after thermal processing all known types of microdefects in crystal are formed. The appearance of microdefects in stratified distribution is due to the thermal processing. The stopping of growth during some interval of time is a modification of actual conditions of growth, i.e. the crystal during this interval receives additional processing.

TEM-researches of areas with A-microdefects is revealed of interstitial dislocation loop with a size 2…20 μm. In the area of crystal with B-microdefects the defects of interstitial type with a sizes 20…60 nm are found (Fig. 2). In the area of crystal with D-microdefects the interstitial defects with a sizes up to 15 nm (Fig. 3) are found.

In case of thermal processing at 800°C the redistribution of defects and increasing their sizes is observed. For processing at 900°C the sizes of D-microdefects is increased up to 10…12 nm. In crystals which processed at 1100°C, together with D-defects, the defects such as sockets with a sizes of 50…100 nm (Fig. 4) were observed.

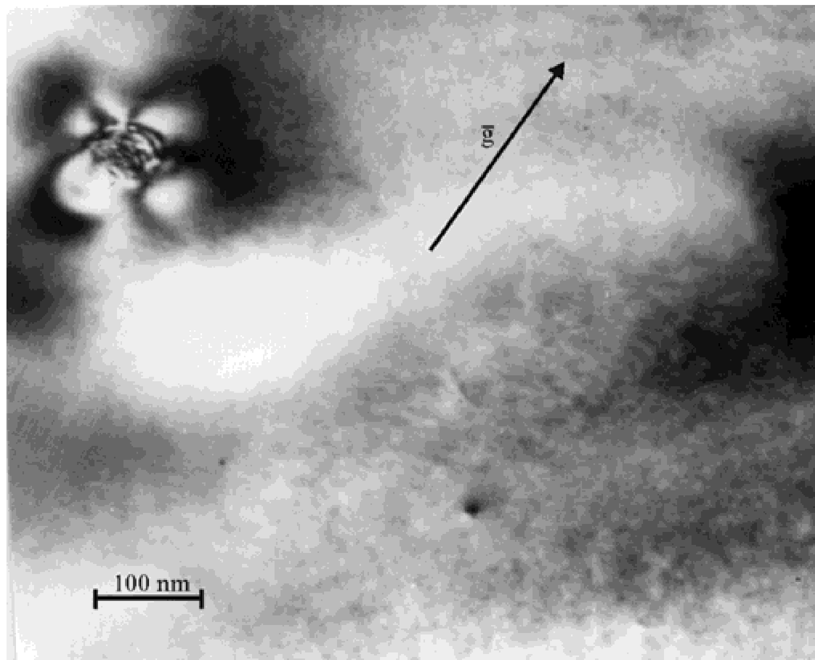

Fig. 4: Defects as "sockets" after crystal thermal processing (V = 6 mm/min, T = 1100 ^{0}C, t = 60 min), dark field, $\bar{g} = (2\bar{2}0)$.

II. On the second stage we investigated the crystals which were obtained at a different growth rates and thermally processed for 3 hours. By TEM was revealed that the crystals before thermal processing contain microdefects as soon as interstitial type (at V ≤ 6 mm/min) and coexisted interstitial and vacancy types (at V > 6 mm/min) (Fig. 5). The TEM-analysis of crystals which were subjected to thermal processing revealed defects with black-white

contrast. In such crystals in comparison with grown-in D-microdefects the size of defects is increased up to 12…15 nm (these defects were marked by us as "small" microdefects). Furthermore, the defects as sockets will be formed (Fig. 4) or even more complicated types with sizes up to 300…700 nm (Fig. 6) (these defects were marked by us as "large" microdefects). This defects are sources of dislocation loops of interstitial type. Completely identical defects (interpreted as B-microdefects) were revealed in crystals of silicon, which were obtained at V = 3 mm/min and were not subjected to thermal processing [16]. TEM-analysis of ours crystals obtained at V = 3 mm/min has shown that these defects are an intermediate stage of development between B- and A-microdefects. The crystals obtained at V ≤ 3 mm/min contain dislocations with a Burgers vector $\overline{b} = 1/2\,[100]$ which are in planes {111}.

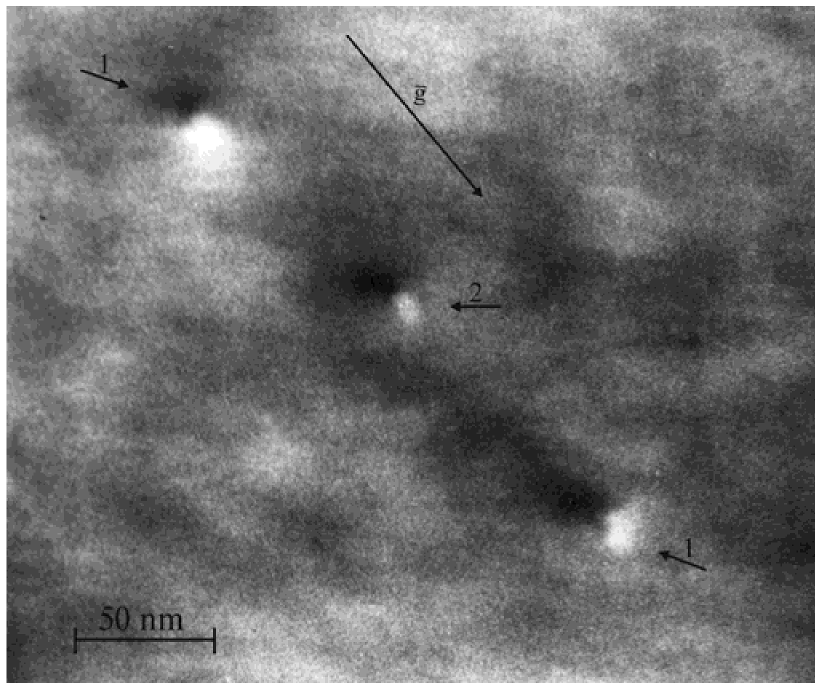

Fig. 5: Defects of vacancy (1) and interstitial (2) type before crystal thermal processing, dark field, $\overline{g} = (\overline{2}20)$.

During thermal processing is generating of "small" microdefects, whereas the concentration of "large" microdefects is lowering with increasing of growth rate. In crystals obtained at V = 8 mm/min the process of interaction of vacancies and interstitials microdefects suppresses formation of "large" microdefects and dislocations [53]. Thus, lowering of the growth rate and the additional thermal processings result in growth and transformation of microdefects.

On Fig. 2b are represented the characteristic square and rhombic form some of B-microdefects. The shape of defects allows to define a their plane and direction of the parties. On a Fig. 2b is shown, that the vector of a diffraction $\overline{g}$ is parallel either party of guadrate or

diagonal of a rhomb. As shown in Ref. [54] such defects faceted with the parties on [110] and [100] and forming on a plane (111) quadrates and rhombs respectively and are in planes {100}. It is possible that the defects have not square form. This defects may have only rectangular form. However because their sizes is very small, the images of defects are shown on a plane (111) as guadrate. The size of B-microdefects is 20…60 nm. It is possible to consider such defects as dislocation loop with a Burgers vector $\bar{b} = 1/2\,[100]$, as shown in [55].

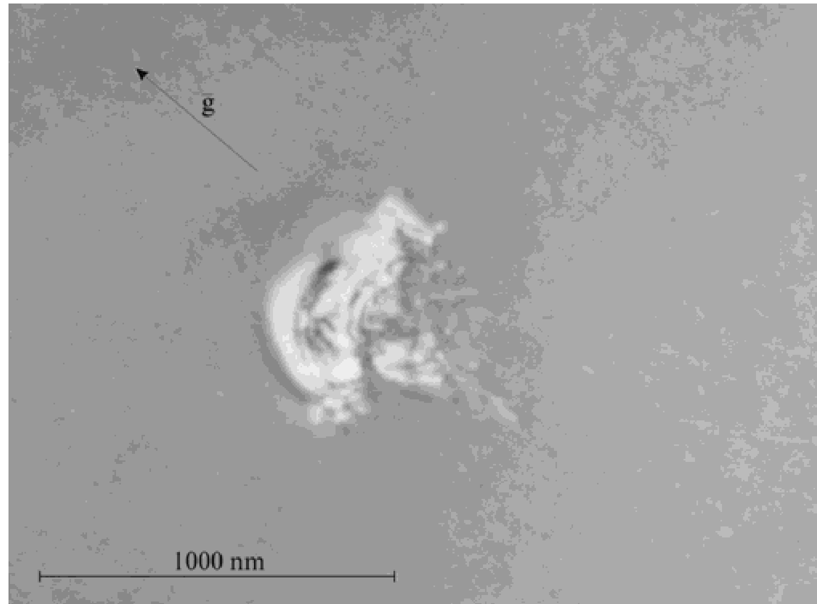

Fig. 6: "Intermediate" defect between B- and A-microdefects, dark field, $\bar{g} = (2\bar{2}0)$.

In Ref. [14] was established that the D-defects give black-white contrast of an image in dynamic conditions, similarly to small dislocation loops. However their geometric structure was not revealed.

It is well known [46, 56, 57] that during the analysis of black-white contrast of small dislocation loops it is possible to use their crystallographic parameters (Burgers vector $\bar{b}$, normal vector $\bar{n}$ to a plane of a dislocation loop). The black-white contrast can be subdivided on internal (size is a diameter of a dislocation loop) and external areas [58]. Such subdividing allows to reveal specific peculiarity of an internal structure of black-white contrast. As shown in Ref. [59] the more complicated internal structure of black-white contrast takes a place for small dislocation loops represented at $|\bar{g}\cdot\bar{b}| > 1$. This internal structure depends on a values of $\bar{g}\cdot\bar{b}$ and does not depend on a diameter of a dislocation loop [59].

As shown in Refs. [60, 61], the direction of a vector $\overline{\ell}$, which describes the contrast change from black to white on an image of defect, will be in parallel projections of a Burgers vector $\overline{b}$ on a image in case of an only boundary dislocation loops, which have the vector of a diffraction $\overline{g}$ also is parallel to a projection of a Burgers vector. In other cases the direction of a vector $\overline{\ell}$ is connected to a direction $\overline{b}$ and $\overline{n}$ to a plane of a loop [60]. In Refs. [59, 60] shown that for boundary dislocation loops and loops with shift components an angle φ_ℓ (angle between vectors $\overline{g}$ and $\overline{\ell}$) as the function of directions $\overline{n}$ and $\overline{b}$ is calculated according to the following formula:

$$\varphi_\ell = \frac{2}{3}\varphi_m , \quad (1)$$

where φ_m is a angle between a vector $\overline{g}$ and projection of average orientation vector $\overline{m}$, which bisects angle between a vectors $\overline{b}$ and $\overline{n}$.

If to analyze of black-white contrast of D-microdefects on microphotos obtained at dynamic conditions ($\overline{g} = [220], \overline{g} = [422]$) that is possible to select three type of contrasts: a) black-white contrast with approximately identical black and white fields; the line of zero contrast is direct; b) black-white contrast with a dominance of one share above other; the line of zero contrast is a polygonal line, and will give an angle of $\alpha \le 90^0$ with the self-parts; c) contrasts as a black point.

From the results of Refs. [58, 61] in which is shown that the detailses of an internal structure of black-white contrast are determined by values $\overline{g} \cdot \overline{b}$, and from our experimental results it is possible to conclude that the observable figures of an image correspond to a) condition $\left|\overline{g} \cdot \overline{b}\right|$ = 0, 2, 4, …; and b) condition $\left|\overline{g} \cdot \overline{b}\right|$ = 1, 3, 5, …; and c) contrast of an image of defect which is lying at centre of a foil. Therefore, it is possible to define a Burgers vector of small dislocation loop. With this purpose it is necessary to define a value $\overline{g} \cdot \overline{b}$ for small loops with $\overline{b} = 1/2[100]$ and $\overline{b} = 1/3[111]$ and $\overline{b} = 1/2[110]$. If to use all probable combinations of values of sets of reflecting planes $\overline{g} = (220)$ and $\overline{g} = (422)$ and also values of Burgers vectors $\overline{b} = 1/2[100]$ and $\overline{b} = 1/3[111]$ and $\overline{b} = 1/2[110]$, then it is possible to conclude that: a) at $\overline{b} = 1/2[100]$ we have $\left|\overline{g} \cdot \overline{b}\right|$ = 0, 1, 2, …; b) at $\overline{b} = 1/3[111]$ we have $\left|\overline{g} \cdot \overline{b}\right|$ = 0, 4/3, 8/3, …; c) at $\overline{b} = 1/2[110]$ we have $\left|\overline{g} \cdot \overline{b}\right|$ = 0, 1, 2, … . Thus, the observable defects can be considered as dislocation loops with Burgers vectors $\overline{b} = 1/2[100]$ and $\overline{b} = 1/2[110]$.

For definition of a planes of dislocation loops it is necessary to measure an angle between a vector of a diffraction $\overline{g}$ and vector of black-white contrast $\overline{\ell}$, i.e. angle φ_ℓ [58]. The experimental values of φ_ℓ and with allowance the data from Refs. [58-61] it is possible to conclude that unknown planes of D-microdefects are the planes {100}, {110}, {111}.

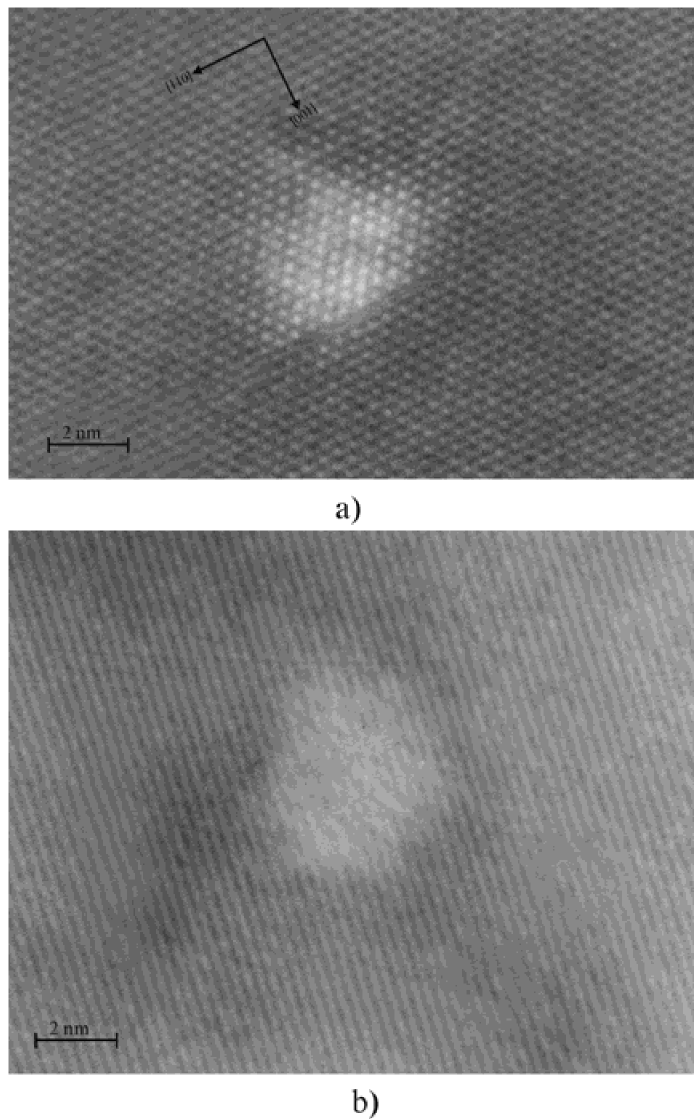

Fig. 7: HREM-image of D-microdefects, (a) - crystalline phase, (b) - amorphous phase.

The quantitative analysis of number of defects with various $\overline{\ell}$ shows that the majority of D-microdefects can be small flat agglomerates of point defects is in planes {100}, i.e. uniformly distributed small B-microdefects. For confirm it can be use a direct image of defects obtained by HREM on electronic microscope JEM-100C (Fig. 7) [14, 20, 27]. A plane of a sample of silicon (112), the crystal is grown at 8 mm/min. The structure of D-microdefects can be consider as crystalline and amorphous. Each of which structures of D-microdefects calls in a crystalline lattice a strain of interstitial type. This defects are similar to defects which were observed in Ref. [55] where was established that defects in amorphous

structure is a SiO_2 microprecipitates. The defects in crystalline ctructure is a SiC microprecipitates [27].

Thus, D-microdefects it is possible to consider as small dislocation loop with Burgers vectors a $\overline{b} = 1/2[100]$ and $\overline{b} = 1/2[110]$ are in planes {100}, {110}, {111}. With a lowering of growth rate the increasing of a size of interstitial D-microdefects is observed (Fig. 8).

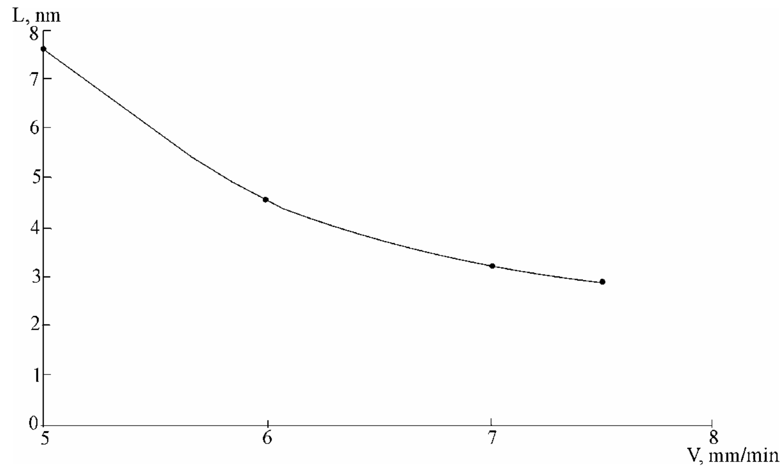

Fig. 8: Experimental dependence a size of interstitial D-microdefects on the crystal growth rate.

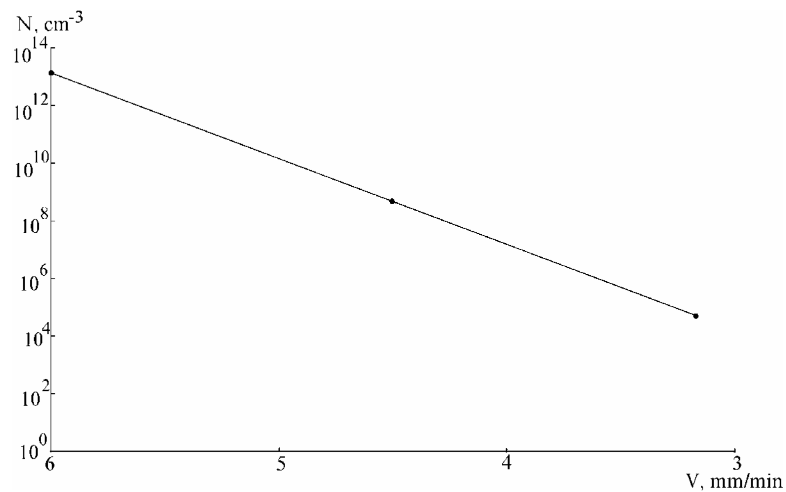

Fig. 9: Experimental dependence of concentration of interstitial microdefects on the crystal growth rate.

On a basis of our experimental data it is possible to suggest the following mechanism of transformation of interstitial microdefects.

Agglomerates are in planes {100} in result is generating of the self-interstitials. The agglomerates of interstitial atoms promote formation and growth of dislocation loops in planes {111}. Thus, D-microdefects which are the predecessors of B-microdefects can exist in two types: as flat agglomerates of point defects in planes {100} and as small dislocation loops in planes {111}. The further growth of agglomerates in planes {100} results in generation of dislocation loops in planes {110}. Such process happens at the expense of the mechanism of prismatic extrusion [62, 63]. In result A-microdefects will be formed as dislocation loops in planes {111} and {110} with a Burgers vector $\bar{b} = 1/2[110]$. Therefore, the transformation of interstitial microdefects proceeds according to following scheme: D-microdefects $\rightarrow$ B-microdefects $\rightarrow$ A-microdefects. During transformation of interstitial microdefects with a lowering of growth rate the size of defects is increased and their concentration decreases (Fig. 9).

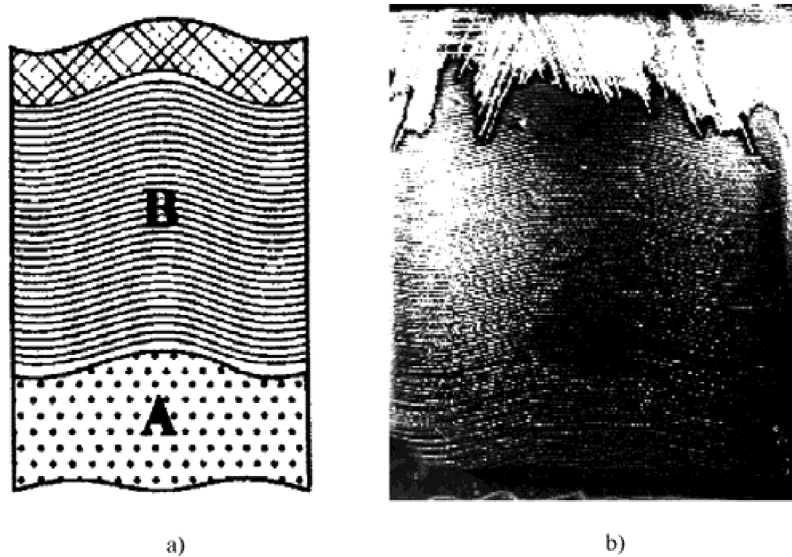

Fig. 10: B- and A-microdefects distribution at V = 3 mm/min after quenching (diameter 30 mm), (a) – schematic representation, (b) – selective etching.

3.2. Influence of a quenching on a structure of silicon single crystals

The experiments with quenching of growing crystals allow to freeze-in the earliest stages of defect formation. The quenching was conducted by decantation of a melting zone which was blowed out by a directed stream of argon. The crystals were grown at growth rates is 2, 3, 6, 9 mm/min. These growth rates, according to the theory [36], should correspond or only "interstitial" (at $V \leq 6$ mm/min) or only "vacancy" (at $V > 6$ mm/min) to regimes of growth. Thus, the revealing of various microdefects during realization of experiment will give a possibility for checks of marked positions. The character of distribution of microdefects and their type were determined after selective etching. These distributions are shown in Fig. 10 and Fig. 11. The quenching experiments allow to confirm the offered mechanism of transformation interstitial microdefects. On Fig. 10 is shown that B-microdefects will formed

before A-microdefects. At the same time D-microdefects (see Fig. 11) formed before B- and A- microdefects.

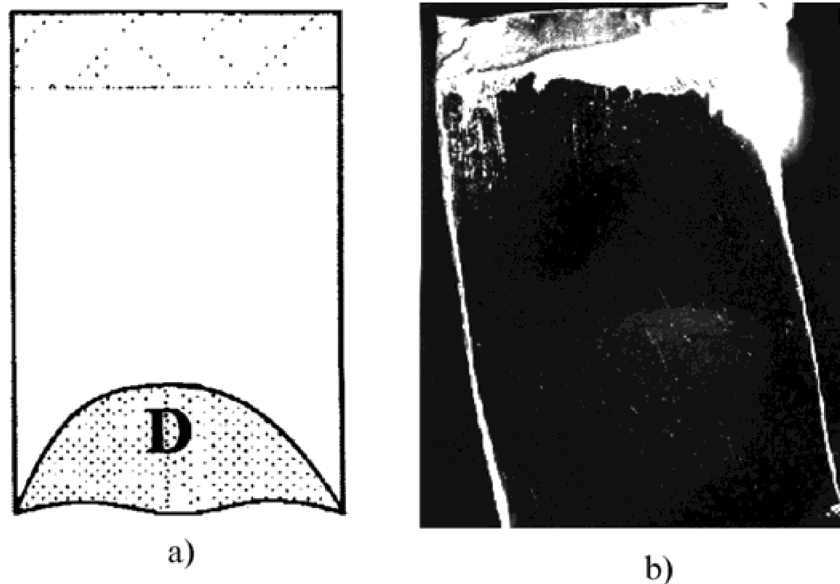

Fig. 11: D-microdefects distribution at V = 6 mm/min after quenching (diameter 30 mm), (a)–schematic representation, (b) – selective etching.

Furthermore, the realization of quenching experiments allows experimentally to define temperatures of formation of microdefects. For A-microdefects as shown in Fig. 10 temperature of formation is equivalent $T_A \cong 1100 \pm 20°C$. On a Fig. 10 also show that B-microdefects will be formed at temperatures close to temperature of smelting. The studies of a surface texture of a separation show that the microdefects are not present at the crystallization front. B-microdefects will be formed at once after a beginning of cooling. Since the area which immediately adjoins to the crystallization front contains dislocations, it is very difficult to determine the beginning of process of formation of B-microdefects. Is possible to suppose that the distance from crystallization front to areas of B-microdefects tending to zero and not exceeding 1…3 mm. Therefore, the best estimate of the temperature of nucleation of B-microdefects that can be made from our data is ≈ 1380 ± 20°C. The distribution of D-microdefects is shown in a Fig. 11. Temperature of formation of D-microdefects is $T_D \cong 1150 \pm 20°C$.

Furthermore, Neimark et al. [64] measured thermal fields which take place during grown of monocrystals of silicon by the thermocouple. They suggested the following emperical formula to describe the dependence of an axial temperature gradient on growth rate of crystal:

$$\frac{dT}{dL} = 10 + (L-16)^2 \cdot \exp(-61.2V - 0.28)\,, \tag{2}$$

where L is a distance from crystallization front, cm; V is a crystal growth rate, cm/s.

The experimental values well coincide with values calculated from (2). The error between of accounts from (2) and experimental values does not exceed ± 2 %.

The results are shows in a Fig. 11 are very important. On a Fig. 11 in the crystal between of crystallization front and area with D-microdefects the so-called "defect-free" area will be formed. According to the theory [36] the formation of such area is correspond of "a condition defect-free crystal" $V/G = C_{crit}$, i.e. the this area divide "interstitial" and "vacancy" areas of crystal on two independent areas. However by TEM-study of "defects-free" area is established that this area is contained simultaneously defects interstitial and vacancy types (Fig. 12). The size of these defects was 2…7 nm and their density was ~ $3.5 \cdot 10^4$ cm^{-2}, whereas the size of D-defects a twice more and density three times less (~$1.2 \cdot 10^4$cm^{-2}). Thus, the "defect-free" area is not "defect-free" and contains small defects of both types of a strain. This result well correlate with results of Ref. [21] where also defects in "defect-free" area were revealed.

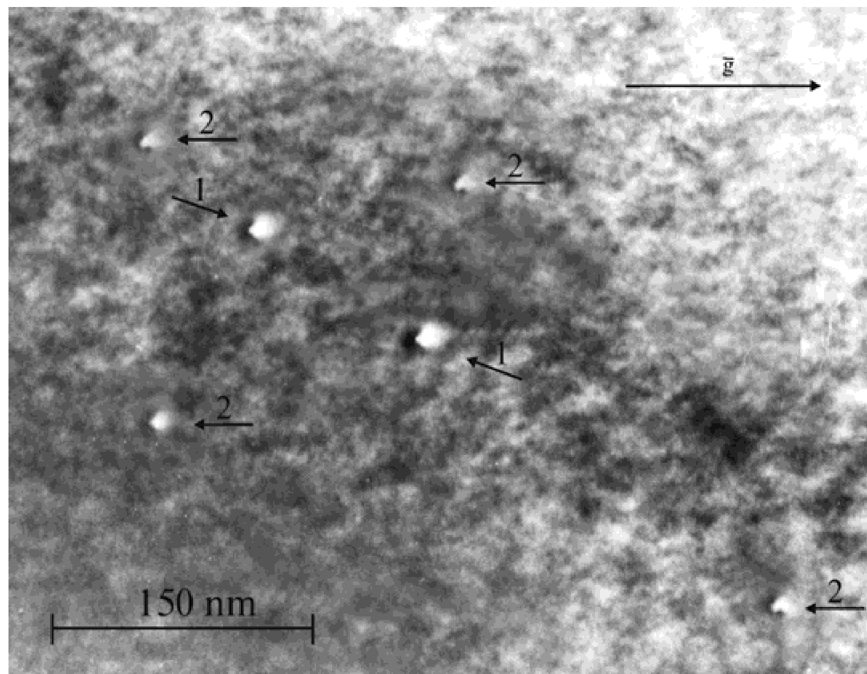

Fig. 12: Defects of vacancy (1) and interstitial (2) type in "defect-free" area, dark field, $\bar{g} = (\bar{2}20)$.

The "defect-free" area of other nature is observed in the crystals grown with a stop of growth (Fig. 1). In this area the defects do not find by selective etching. This area is transitional area between uniformly distributed D-microdefects and B-microdefects which is stratified distribution. Thus, this area is not a "defect-free" area which is represented in Fig. 11. In this area only interstitial D-microdefects is observed.

Furthermore, temperature of formation of interstitial D-microdefects T = 1150°C well correlates with temperature of a dissociation D-microdefects [32, 65]. However in Refs. [32, 65] were investigated CZ-Si in which, according to [17], D-microdefects had a vacancy

nature. Therefore, if not to use a disputable nomenclature about "D-microdefects" we may say that in Refs. [32, 65] temperature of formation of interstitial D-microdefects was determined. This position is well correlates with results of our quenching experiments.

We also studied the crystal which grown at V = 9 mm/min. According to [36] this crystal should contain only vacancy microdefects because grows in a "vacancy" regime. However TEM-studies shown of microdefects of vacancy and interstitial types which are approximately in equal concentration. Thus, the our researches to confirm of all positions in Refs. [14, 18-21, 25].

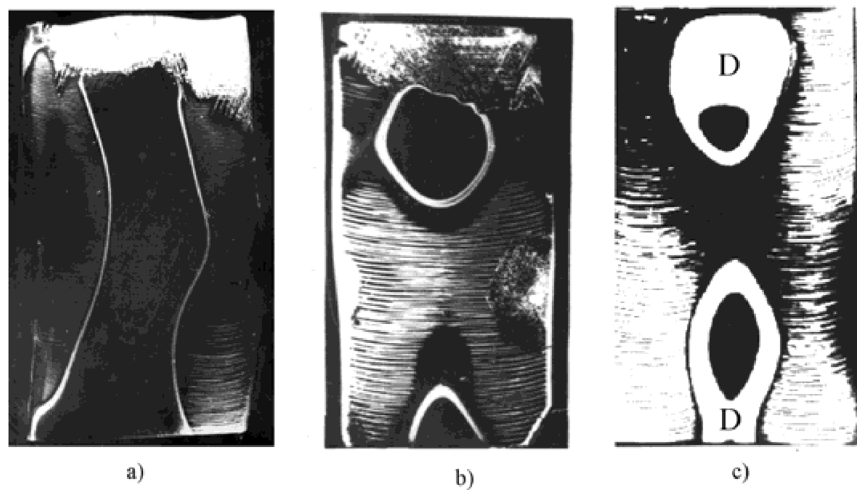

Fig. 13: The defects transformation in thermal processed crystal at V = 4 mm/min (diameter 30 mm), (a)– growth with the additional heating, (b) – microdefects after additional thermal processing (T = 1200 ^{0}C, t = 20 min), (c) – the emerging of D-microdefects after oxygen doping.

3.3. Influence of a growth condition and impurities on a defect formation process

During growth of crystal the fluctuations of growth rate take place [15]. The periodic modifications of growth rate result in periodic modifications of concentration of impurities, in particular of carbon. Local maxima in concentrations of A- and B-microdefects coincide with the areas with high concentration of phosphors [66]. As the heterogeneities of distribution of phosphors and carbon are similar [67] the conclusion was made that the formation of microdefects should happen including of atoms of carbon [12, 28]. Föll et al. [28] has established that the concentration of microdefects is increased with increasing carbon contents. Therefore, stratified distribution of microdefects indicates heterogeneous character of their nucleation. This result is well correlate with data of Ref. [26]. Such impurities as oxygen [37, 55, 68-73] and carbon [12, 28, 67, 74-78] which are found in high concentrations in FZ silicon [79] render direct effect on process of formation of defects.

To confirm the influence of oxygen atoms on formation of microdefects the crystal at V = 4 mm/min with a simultaneous additional heating of a growing part was obtained. Usually at

4 mm/min will be formed B-microdefects, but in this case additional heating has reduced a temperature gradient and was formed at centre of crystal of "defect-free" area (Fig. 13a), i.e. area containing of vacancy and interstitial defects. Then crystal cutted on two half. After cutting the average part of each half of crystal was treated at T = 1200°C during 20 min by a additional inductor. This thermal processing give a rupture of the "defect-free" channel and was formed bands of B-microdefects (Fig. 13b). By IR-absorption was define that in a place of emerging of B-microdefects the concentration of carbon is $5{\cdot}10^{16}$ cm^{-3} and oxygen is less $2{\cdot}10^{16}$ cm^{-3}. Thus, experiment has confirmed as process of transformation of microdefects as participation of carbon in the process of formation of B-microdefects.

After doping by oxygen from a gas phase D-microdefects will be formed and the concentration of B-microdefects is increased. After doping concentration of B-microdefects was $2\ldots6{\cdot}10^{5}$ cm^{-2} while before doping the concentration was $1\ldots2{\cdot}10^{4}$ cm^{-2} (Fig. 13c).

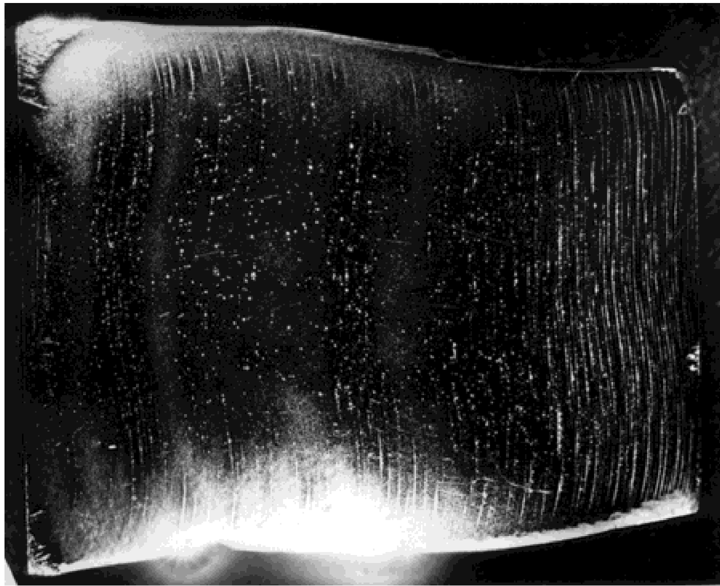

Fig. 14: B- and A-microdefects distribution in a crystal grown with a variable growth rate (diameter 30 mm).

Thus, the emerging of D-microdefects because of a shrinking of "defect-free" area which contains very small microdefects of vacancy and interstitial types shows that these both type of microdefects are the predecessors of D-microdefects, i.e. their nuclei. In case of the large contents of oxygen in FZ-Si (more than 10^{16} cm^{-3}) the formation of pairs vacancy-interstitial atom of oxygen is favourable [80]. Therefore, in the present case nuclei of D-microdefects probably are the complexes of vacancies and interstitial oxygen atoms O_i. It is possible that is complexes a [VO_2] which are detected in silicon during the radiation experiments [81, 82].

To determine the influence of self-interstitials on formation of B- and A-microdefects the crystal with variable growth rate was obtained. The growth rate decreased by steps $\Delta V = 0.5$

mm/min from V = 3 mm/min to V = 0.5 mm/min (Fig. 14). As shown in a Fig. 14 at V = 2 mm/min revealed large uniformly distributed A-microdefects, which are dislocation loops with sizes up to 20 μm. However, stage change of growth rate results in formation of uniformly distributed "clouds" of defects with sizes smaller than at A-microdefects (r_A = 70…120 μm, r_B = 10…15 μm) and densities greater than at A-microdefects ($N_A = 4\cdot10^2$ cm^{-2}, $N_B = 1{,}3\cdot10^4$ cm^{-2}). The fluctuations of growth rate result in increasing concentration of self-interstitials [83]. For high concentration of self-interstitials the size of nuclei of microprecipitates SiO_2 is increased [84]. But at low growth rates the atoms C_s play a catalytic role in formation of centres of precipitation [51, 85]. Thus, the complexes will be formed which consist of atoms of carbon and interstitial atoms of silicon ($C_s + I_{Si} \leftrightarrow [C_sI_{Si}]$). In result will be formed B-microdefects in a uniform distribution.

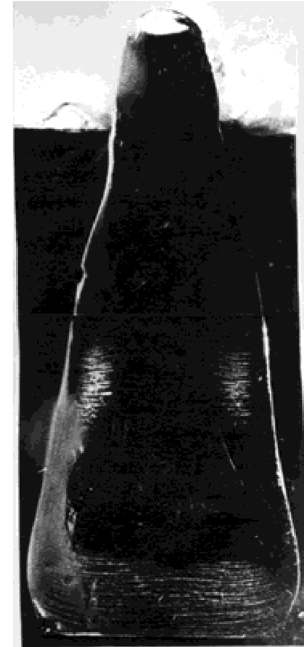

Fig. 15: A- and B-microdefects distribution at a gradual lowering the crystal diameter (the initial diameter 30 mm).

Thus, the experiments about influence of impurities to process of defect formation in silicon are confirm a heterogeneous character nucleation of microdefects.

With the purpose of study of influence of crystal growth conditions on a types of formed of microdefects the following experiments were conducted.

Were grown crystals at a constant growth rate V = 3 mm/min with a gradual lowering of a diameter in one group of crystals from 30 mm in the beginning up to 15 mm in an finish, and in other group from 50 mm in the beginning up to 25 mm in an finish. Thus, the shape of obtained crystals was not cylindrical, but it was conic. With a lowering of a diameter the cooling rate of crystals is increased. This process is responsible for formation of microdefects of more and more smaller sizes. Really with a lowering of a diameter instead of A-microdefects the B-microdefects in both groups of crystals were observed. The sites of

crystals which were close to top of a cone was a "defect-free" (Fig. 15). Therefore, is established that minor modification of a diameter of crystal at a constant growth rate is similar of increase of growth rate and results to vanishing A-, and then B-microdefects.

Furthermore, the crystal at a high growth rates V = 5, 6, 7, 7.5, 9 mm/min was obtained. In sites of the crystal which grown at V = 5…6 mm/min by selective etching were detected D-microdefects which are uniformly distributed as the channel in a central part of crystal (Fig. 16a). By IR-absorption the contents of carbon in the channel ~ $4.4\cdot10^{16}$ sm^{-3} and outside of the channel ~ $2\cdot10^{16}$ cm^{-3} respectively.

In sites of crystal which were grown at a 7 and 7.5 mm/min we observed the widening of the channel in a ring because of formation in centre of so-called "defect-free" area (Fig. 16b, c). Thus, at gradual increasing of growth rate we observed ruptured channel with D-microdefects. It was observed that ring on an edge of crystal which with further increasing of growth rate is shrinking and then disappeared. We conducted TEM-researches of crystals shown in a Fig. 16. Were shown that in channel the all defects was black-white contrast similarly to small dislocation loops, i.e. as defects of interstitial type. The concentration of microdefects in the channel ~ 10^{13} cm^{-3}, size of defects ~ 5…6 nm.

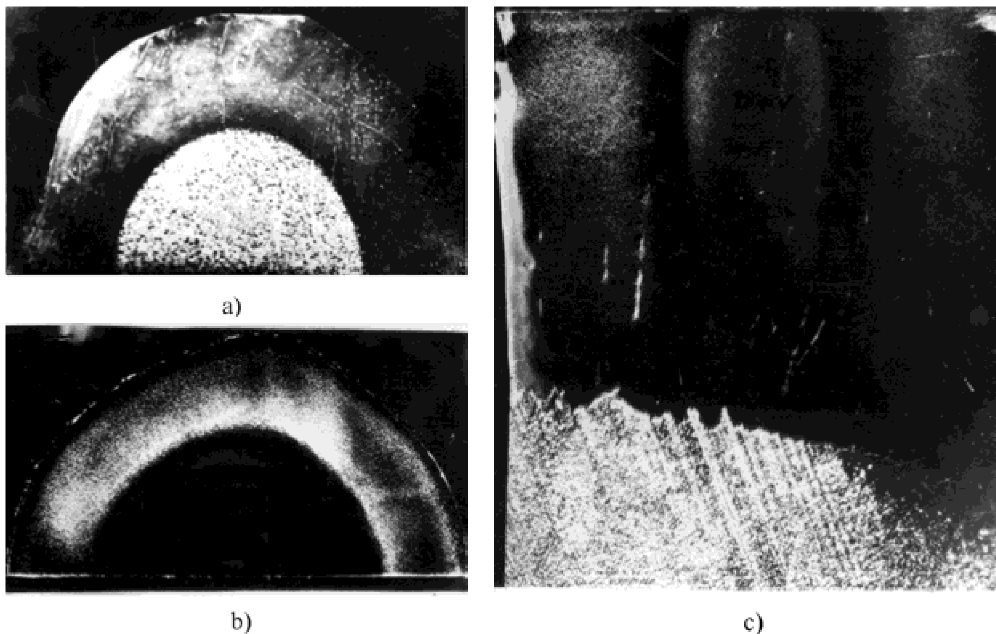

Fig. 16: D-microdefects distribution on a dependence of crystal growth rate (diameter 30 mm), (a)-distribution as a "channel" at 6 mm/min, (b)-and (c)-distribution as a "ring" at 7.5 mm/min.

TEM-researches were conducted for a site with ring distribution of D-microdefects. In the area of a ring the defects of identical contrast, size and concentration were found as in the area of the channel of D-defects, i.e. only interstitial type. Inside a ring the jointly coexisted microdefects of vacancy and interstitial types were detected.

For further increase of growth rate of crystal a diameter of a ring of D-microdefects the gradually is shrinks, and at 9 mm/min the ring disappears. Thus, in the crystal which were grown at 9 mm/min are observed uniformly distributed defects of vacancy and interstitial types. This defects is a approximately identical concentration.

4. The nucleation, growth and further transformation of microdefects in FZ-Si

Thus, the experiments have shown that the nucleation and growth of microdefects depends on conditions of crystal growth (growth rate of crystal, cooling rate and temperature gradient) and on concentration of impurities of carbon and oxygen. Therefore, it is possible to offer a qualitative model of formation, growth and transformation of microdefects in dislocation-free single crystals FZ-Si.

The analysis of literary data and the experiments in the present paper show a significant role of self-interstitials in high-temperature experiments. All known types of microdefects in FZ-Si (i.e. A-, B-, D-defects) have an interstitial nature. Furthermore, for research of a gold diffusion in silicon was shown that the atoms of gold take in silicon substitutional (Au_s) and interstitial position (Au_i). The diffusion of gold in silicon is not explained with the help of Frank-Turnbull mechanism ($Au_i + V \leftrightarrow Au_s$) [86], but logic explanation may be given in kick-out mechanism [87-90]: $Au_i \leftrightarrow Au_s + I$.

Also we have the experimental results that the significant role is played vacancies [33, 91, 92]. Thus, the correlation of thermodynamic accounts and experimental data is possible only in model which is supposing coexistence of self-interstitial and vacancies in a thermal equilibrium at high temperatures [92, 93]. In this model diffusivity of impurity is the sum of diffusivities on interstitials and on vacancies [92]. In Ref. [94] theoretical models of a self-diffusion in silicon with simultaneous participation of self-interstitials and vacancies were offered. Was shown [94] that interstitial and vacancy contributions to a self-diffusion are equalized close 1100 ^{0}C and for higher temperatures during a self-diffusion the self-interstitials dominate whereas for a lower temperatures the vacancies dominate. The results obtained in Refs. [95, 96] is particularly confirm this model.

With the help of our TEM-researches it is established that vacancy microdefects occur together with interstitial microdefects in crystals grown at $V > 6$ mm/min. A ratio of vacancy and interstitial microdefects in samples obtained at $V = 7.5$ mm/min is approximately $\approx 1 : 4$. In crystals obtained at $V = 9$ mm/min, interstitial and vacancy defects coexist approximately in identical concentration, i.e. $\sim 1 : 1$. Thus, the critical growth rate of crystal for which vacancy microdefects occur is in the interval of 6 mm/min < V < 6.5 mm/min (Fig. 17).

If the concentration of vacancy and interstitial microdefects are approximately identical, it is possible to assume that for equilibrium conditions of vacancies and self-interstitials exist simultaneously and also in approximately identical concentration. The estimates from Ref. [36] give concentration of vacancies at the temperature of smelting are $1.5 \cdot 10^{14}$ cm^{-3}, but self-interstitials are $1.3 \cdot 10^{14}$ cm^{-3}.

In the Voronkov theory [36] it is suggested that the main role in an initial stage of disintegration oversaturation solid solution of point defects is played by process of a recombination between vacancies and self-interstitials.

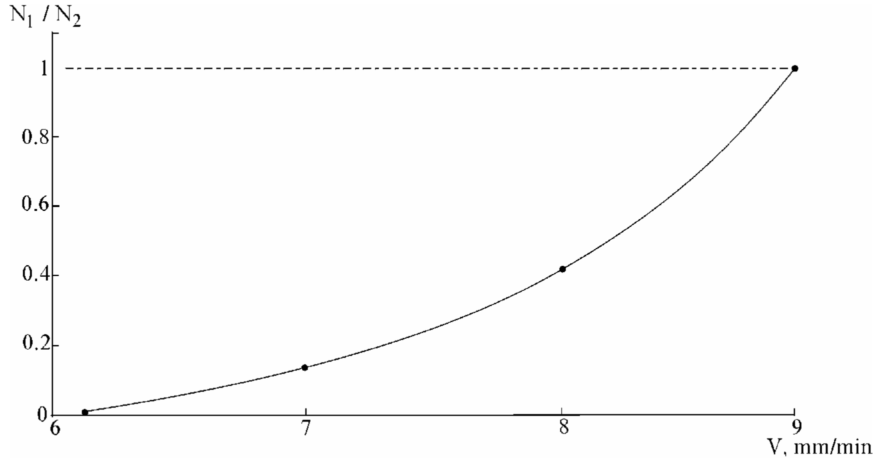

Fig. 17: Experimental dependence of the ratio of concentration of vacancy (N_1) and interstitial (N_2) microdefects on crystal growth rate.

However in Refs. [13, 33, 97] it was supposed that the direct recombination between vacancies and self-interstitials is hampered by the existence of an energy barrier. Tempelhoff et al. [13, 97] argued that the recombination takes place only on some centres (B- and A-microdefects, dislocations, surface of crystal), and the direct recombination is impossible. In Refs. [34, 98, 99] it was discussed the theory of energy barrier which is hampered of direct recombination between vacancies and self-interstitials.

In the Ref. [34] the local equilibrium was considered

$$C_I C_V = C_I^{eqv} C_V^{eqv}, \tag{3}$$

where is a C_V is concentration of vacancies; C_I is a concentration of self-interstitials.

The order of values for time during the system will achieve an equilibrium if the recombinational barrier is absence calculation according to the formula:

$$\tau \le \frac{\Omega}{4\pi D^S r_0}, \tag{4}$$

where is the Ω is a volume of elementary cell; D^S is a constant of a self-diffusion; r_0 is a recombination cut.

Estimates from Ref [99] at a $D^S = 10^{-15}$ cm^2/s, $T = 1100$°C, $r_0 = 5\cdot10^{-8}$ cm give the values $\tau \le 0.05$. This value was in 10^5 less experimentally observable values [99]. Thus, the conclusion was made that the recombination is determined not by a diffusion, but overcoming of a recombinational barrier exceeding free energy of a diffusion on ΔG. The value 10^5 arises from the Boltzmann factor $(\exp \Delta G / kT)$.

In Ref. [99] it was supposed that a recombinational barrier is enthalpy barrier and entropy component TΔS is very small:

$$\Delta G = \Delta H - T\Delta S \tag{5}$$

However in Ref. [100] was remarked that the intrinsic point defects behave variously for the various temperatures. Hence, the fluctuations of barrier values take place whereas the barrier $\Delta H = 1.4\ eV$ was considered to constants [99].

Was established that the barrier will be increased with increase of temperature [100]. Thus, the conclusion was made that the recombinational barrier is determined as entropy component from the equation (5) [100].

The microscopic model of entropy barrier in details was discussed in Refs. [88-90, 101-106]. According to this model the point defects in silicon (vacancies and self-interstitials) have an extended character at very high temperatures, i.e. one atom (or one vacancy) are extended on some nuclear volumes (11 atoms occupied 10 cells). In this model the recombination happens only for of "simultaneous compression both from these defects in a neighbourhood of one nuclear volume" [100]. The extended defect configurations have the greater number of microstates than point defect. Thus, the compression lowered an entropy and therefore the entropy barrier $\Delta S < 0$ exists. If temperature is lowering the barrier is considerably reduced and disappearing at low temperatures when the defects easily recombine. Thus, the intrinsic point defects at a high temperatures are extended, but at a low temperatures they have the dumbbell configuration [100, 107]. The theory of extended defect configurations and recombinational barrier was confirmed in Refs. [108-113].

Thus, according to the theory [100] which was constructed in the correspondence with the Ref. [94] in silicon at high temperatures the joint coexistence of both types of intrinsic point defects in equivalent concentration is observed. This fact determine the values of a self-diffusion factor. Furthermore, "the condition of a smallness" should be taken into account:

$$\Delta H << |T\Delta S| \tag{6}$$

In Ref. [100] on results of oxidizing experiments and from the value $\exp(\Delta G/kT) = 10^5$ the barrier was estimated as $\Delta S = 11.5k$ at T = 1373 K.

The our accounts according to (5)-(6) give the value of a barrier at T = 1685 K (temperature of smelting) as $\Delta G = 1.674\ eV$.

Hence, the estimate of value τ from the equation (4) needs with allowance of a recombinational barrier, i.e.:

$$\tau \le \frac{\Omega}{4\pi D^S r_0 \cdot \exp(-\Delta G/kT)} \tag{7}$$

The allowance of a barrier value ΔG gives the value of $\tau \approx$ 53 min. Thus, for standard sizes of ingots and standard time of its growth the recombination will have no time to come true.

Therefore, we can estimate the length of area near to crystallization front on which the recombination happens according to [36]:

$$\ell = \frac{2kT_m^2}{(\Delta H_i + \Delta H_v)G}\ , \tag{8}$$

where is the k is a constant Boltzmann; T_m is a temperature of smelting; G is a axial temperature gradient; ΔH_i and ΔH_v are energy of self-interstitial and vacancy formation respectively.

The value of G we can define from the equation (2) with allowance that the gradient is defined on crystallization front:

$$G_{L=0} = 10 + 256\exp(-61.2V - 0.28) \quad (9)$$

We did account for crystal which was grown at V = 9 mm/min when the equality of concentration of vacancy and interstitial microdefects was established. Thus, from the equations (8)-(9) and at T_m = 1685K, $\Delta H_i \approx \Delta H_v = 4.5\ eV$, V = 9 mm/min is established that $\ell = 6.25\ mm$.

Then time during the intrinsic point defects exist in recombinational area is define from the following equation:

$$t = \frac{\ell}{V}, \quad (10)$$

where is V – growth rate of crystal. At V = 9 mm/min is established that t = 41.6 s. The accounts from equations (7)-(10) give at V = 2 mm/min the following values: $\ell = 3.25\ mm$ and $t = 1.625$ min The results [36] show at V = 2 mm/min the following values: $\ell = 2\ mm$, $t = 1$ min and $\tau \approx 0.3\ s$.

We received the differences in accounts from the theory [36]. It is possible because of that in Ref. [36] the theory of enthalpy barrier is used and is used that the joint coexistence of both types of intrinsic point defects is denied. According to [36] τ should exist separately for "interstitial" and separately for "vacancy" of growth regimes, i.e. according to [114]:

$$\begin{aligned} \tau_i &\approx \frac{1}{4\pi r D_i C_i \exp(-\Delta H/kT)} \\ \tau_v &\approx \frac{1}{4\pi r D_v C_v \exp(-\Delta H/kT)} \end{aligned}, \quad (11)$$

where is D_i and D_v is a diffusivities of a self-interstitials and vacancies respectively; C_i and C_v is a concentration of self-interstitials and vacancies respecrively.

However experimental results in the Refs. [14, 18-27, 39, 40] and our results confirm the fact of joint coexistence of microdefects with various sign of a straine and the fact of joint coexistence of intrinsic point defects. These results can be estimated only in theory of joint coexistence of intrinsic point defects [94] and theory of entropy barrier [100]. According to the theory [94] in the equation (7) the factor of a joint self-diffusion of vacancies and self-interstitials is taken into account.

Thus, the experimental results which are in the good correlation with theoretical datas allows to approve that at the temperature of smelting in dislocation free silicon single crystals take a place simultaneous coexistence of equilibrium concentration of vacancies and self-interstitials. Concentration of vacancies and self-interstitials are approximately identical near to the crystallization front. The recombination between them in an initial stage of their interaction at a high temperatures is hampered by entropy barrier. Thus, the disintegration of oversaturation solid solution of intrinsic point defects proceeds simultaneously on two mechanisms: vacancy and interstitial. The microdefects are formed in result of interaction of intrinsic point defects with impurities of oxygen and carbon.

For vacancy mechanism theoretically is possible only vacancy aggregation and joint vacancy-impurities aggregation [36]. Vacancy-impurities aggregation begins earlier than only a vacancy aggregation. Interstitial atoms of oxygen are very mobile and therefore the formation of complexes is simulated by a leaving of interstitial oxygen in positions of substitution O_s:

$$O_i + V_{Si} \rightarrow O_s \rightarrow 2O_s + 3O_s + \ldots + nO_s.$$

At lower temperature O_s can be centres of formation of microprecipitates of oxygen. It is possible to estimate the concentration of oxygen precipitates [37]:

$$N \approx \frac{C_v}{4\pi\gamma^2}\left(\frac{\rho n_{cr}}{\eta}\right)^{1/2}\left(\frac{E_{cr}\left|V_c\right|}{DCkT^2}\right)^{3/2}, \tag{12}$$

where is C_v is a concentration of vacancies; ρ is a density of silicon knots; n_{cr} is a nuclei critical size; C is a concentration of oxygen; D is a diffusivity of oxygen; E_{cr} is a energy of connection on one atom of oxygen; V_c is a cooling rate.

For FZ-Si at $C_v \sim 10^{14}$ cm^{-3}, $C \sim 10^{16}$ cm^{-3}, $D \sim 10^{-9}$ cm^2/s we shall receive $N \sim 5 \cdot 10^{12}$cm^{-3}. Direct TEM-researches of vacancy and interstitial microdefects given the values of their concentration ~ 10^{13} cm^{-3}.

When will be formed microprecipitates there is a surplus of volume and one vacancy will be consumed by a growing precipitate for each two oxygen atoms precipitated. The aggregation is accompanied by issue of atoms I_{Si}. The absorption of vacancies and impurity by growing microdefects results in a decreased concentration of vacancies in a comparison with concentration of oxygen. In result precipitates begin to absorb oxygen without participation of vacancies their sizes are increased and then the type of a strain around them varies from vacancy (tensile) to interstitial (compressive). The similar results were obtained by HREM in Refs. [112, 115] The boundary of full transition can be determined from the relation V/G. Thus, the parameter C_{crit} of the theory [36] does not describe a condition of change of growth regimes ("interstitial" or "vacancy"). This parameter describes conditions of emerging (or vanishing) of microdefects of a vacancy type in an result of a diffusion and interaction of point defects during cooling of crystal. It is possible to define C_{crit} for critical growth rate (Fig. 17). At V = 6.25 mm/min we shall receive $C_{crit} = 9.31 \cdot 10^{-5}$ cm^2/(s·K).

The centers of nucleation on a base of interstitial atoms of oxygen exist also for the interstitial mechanism. However here catalytic role is played by carbon atoms. Oversaturation of interstitial atoms of silicon results in appearance of complexes $[C_sI_{Si}]$:

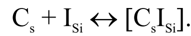

$$C_s + I_{Si} \leftrightarrow [C_sI_{Si}].$$

The number of interstitial defects can be account from the equation [37]:

$$N \approx 0.13\left(\frac{\rho}{C_i}\right)^{1/2}\left(\frac{E_{cr}\left|V_c\right|}{D_i kT^2}\right)^{3/2}, \qquad (13)$$

where is C_i is a concentration of self-interstitials before condensation; E_{cr} = 1.5 eV is a energy of connection of a critical nuclei on one atom of silicon.

The estimate for C_i ~ 10^{14} cm^{-3} and D_i ~ $3.5\cdot10^{-4}$ cm^2/s gives the value N ~ 10^6 cm^{-3}. The similar value is obtained by TEM-researches of A-microdefects concentration.

Lowering of a critical radius $[C_sI_{Si}]$-nucleis and acceleration of a diffusion C_s here happens. As the result agglomerates $[C_sI_{Si}]$ will be formed. Furthermore, during supersaturation of I_{Si} co-precipitation of O_i and C_s can happen [77, 116-119]. Thus, for formation of B-microdefects:

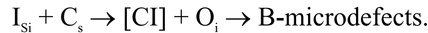

$$I_{Si} + C_s \rightarrow [CI] + O_i \rightarrow \text{B-microdefects}.$$

The growth of interstitial microdefects results in a significant lowering of self-interstitials concentration. It creates conditions for precipitations of impurity. In this case formation of particles of a impurity phase is accompanied by generation of self-interstitials in positions between knots of the lattice. In an result two types of interstitial microdefects will be formed: as interstitial agglomerates (drains for interstitial atoms of silicon) and as impurity precipitates (sources of these atoms).

Both mechanisms (vacancy and interstitial) result in formation of small interstitial agglomerations, i.e. D-microdefects. The confirm of this position obtained by HREM. Were revealed two types of image of D-microdefects: as agglomerates of atoms with a crystalline structure and as agglomerates of atoms with amorphous structure (Fig. 7) [14, 20, 27]. In Ref. [20] was shown that "amorphous" images give microprecipitates amorphous SiO_2 phase. Crystalline structure may be is a SiC precipitate [27]. Both types of D-microdefects are defects of interstitial type. This D-microdefects are uniformly distributed B-microdefects. The B-microdefects is transformed in A-microdefects.

These mechanisms are described by the following equations.

<u>For vacancy mechanism:</u>

a) $nO_i + V_{Si} \rightarrow n(VO_2) \rightarrow$ vacancy microdefects.

b) $n(VO_2) + O_i + ... + nO_i \rightarrow n[(V_mO_n) + I_{Si}] \rightarrow$ D-microdefects.

<u>For interstitial mechanism:</u>

a) $C_s + I_{Si} \rightarrow (C_sI_{Si}) \rightarrow$ D-microdefects.

b) $(C_sI_{Si}) + O_i \rightarrow n[(C_sI_{Si}) + O_i] \rightarrow$ B-microdefects.

c) B-microdefects + $I_{Si} \rightarrow$ A-microdefects.

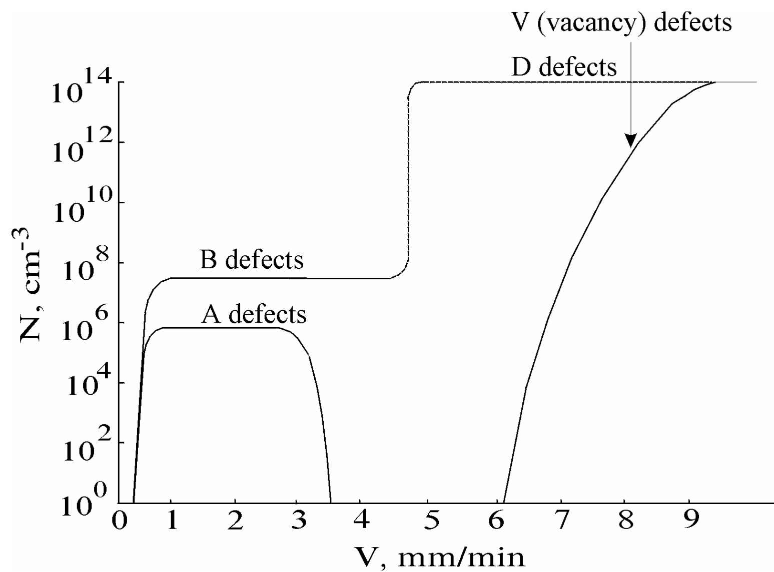

Fig. 18: Schematic diagram of formation and transformation of microdefects in FZ-Si crystals.

On Fig. 18 the scheme of microdefects formation process in FZ-Si is shown.

5. Conclusions

Thus, the formation of vacancy and interstitial microdefects is due by disintegration of oversaturation solid solution of intrinsic point defects. All known types of microdefects are formed in result of interaction of intrinsic point defects with impurities of oxygen and carbon. Concentration of vacancies and self-interstitials are approximately identical near to crystallization front. The recombination between them in an initial stage of their interaction at a high temperatures is hampered. Therefore, the formation of microdefects proceeds simultaneously on two mechanisms: vacancy and interstitial. Vacancy and interstitial microdefects coexist in crystal. The parameter $V/G = C_{crit}$ describes conditions of emerging (vanishing) of vacancy microdefects in crystal.

Thus, the Voronkov model requires a following clarifications:

a) The recombination between vacancies and self-interstitials for temperatures close to temperature of smelting is not present.
b) Primary grown-in microdefects are vacancy and interstitial defects.
c) In the "vacancy area" of the crystals which grown in "vacancy" regime of growth contains simultaneously interstitial and vacancy defects in identical concentration.

These positions were made for FZ-Si. However mechanism microdefects formation in both types of crystals FZ-Si and CZ-Si are similar. We have made this supposition in the Refs. [27, 120] and we shall represent our results in the new paper.

Acknowledgements

The authors are very grateful to the board of Zaporozhye Titan-Magnesium Plant for the help in deriving the crystals. The authors want to thank Dr. A.V. Koval'chuk for providing the possibility of using of the necessary equipment. Authors are very indebted to Dr. Taketoshi Hibiya for him interest to present paper and help for our difficulties.

References

[1] A.J.R. de Kock: Phil. Res. Rep. (1973) 1.
[2] N.V. Veselovskaya, E.G. Sheikhet, K.N. Neimark and E.S. Falkevich: in Rost i legirovanie poluprovodnikovykh kristallov i plenok, vol. 2 (Nauka, Novosibirsk, 1977) p. 284.
[3] H. Nishikawa, T. Tanaka, Y. Yanase et al.: Jpn. J. Appl. Phys. 36 (1997) 6595.
[4] H.C. Gatos: in Defect Control in Semicond., vol. 1 (Elsevier, Amsterdam, 1990) p. 3.
[5] T. Abe: JAERI-M 92 (1993) 7.
[6] T. S. Plaskett: Trans. Met. Soc. AIME 233 (1965) 809.
[7] T. Abe, T. Samizo and S. Maruyama: Jpn. J. Appl. Phys. 5 (1966) 255.
[8] H. Hattori and N. Kato: J. Phys. Soc. Jpn. 21 (1966) 1773.
[9] J. Chikawa, Y. Asada and I. Fujimoto: J. Appl. Phys. 41 (1970) 1922.
[10] A. J. R. De Kock: Appl. Phys. Lett. 16 (1970) 100.
[11] A. J. R. De Kock: J. Electrochem. Soc. 118 (1971) 1851.
[12] H. Föll and B.O. Kolbesen: J. Appl. Phys. 8 (1975) 319.
[13] K. Tempelhoff and N. Van Sung: Phys. Stat. Sol. (a) 70 (1982) 441.
[14] A.A. Sitnikova, L.M. Sorokin, I.E. Talanin et al.: Phys. Stat. Sol. (a) 81 (1984) 433.
[15] T. Abe, H. Harada and J. Chikawa: Physica 116 B/C (1983) 139.
[16] P. M. Petroff and A. J. R. De Kock: J. Cryst. Growth 30 (1975) 117.
[17] P.J. Roksnoer and H.M.B. Van den Boom: J. Cryst. Growth 53 (1981) 563.
[18] A.A. Sitnikova, L.M. Sorokin, I.E. Talanin et al.: Phys. Stat. Sol. (a) 90 (1985) K31.
[19] A.A. Sitnikova, L.M. Sorokin, I.E. Talanin et al.: Fizika Tverdogo Tela 28 (1986) 1829.
[20] A.A. Sitnikova, L.M. Sorokin and E.G. Sheikhet: Fizika Tverdogo Tela 29 (1987) 2623.
[21] V.T. Bublik and N.M. Zotov: Cryst. Rep. 42 (1997) 1033.
[22] S. Iida, Y. Aoki, Y. Sugita et al. : Jpn. J. Appl. Phys. 37 (1998) 241.
[23] Y. K. Kim, S. Ha Tae and J. K. Yoon: J. Mater. Sci. 33 (1998) 4627.
[24] N. Nango, S. Iida and T. Ogawa: J. Appl. Phys. 38 (1999) 5695.
[25] V.I. Talanin: in Siberian Russ. Workshops on Electron Devices and Materials (EDM'2000). Proc., (NSTU, Novosibirsk, 2000) p. 87.
[26] S. Iida, Y. Aoki, K. Okitsu et al.: Jpn. J. Appl. Phys. 39 (2000) 6130.
[27] V.I. Talanin, I.E. Talanin and D.I. Levinson: in Proc. of ICSC-01 (Obninsk, 2001) p. 202.
[28] H. Föll, U. Gösele and B.O. Kolbesen: J. Cryst. Growth 40 (1977) 90.
[29] T.Y. Tan and U. Gösele: Appl. Phys. A 37 (1985) 1.
[30] J. Chikawa and S. Shirai: J. Cryst. Growth 39 (1977) 328.
[31] J.A. Van Vechten: Phys. Rev. B 17 (1978) 3197.
[32] P.J. Roksnoer: J. Cryst. Growth 58 (1984) 596.
[33] S. M. Hu: J. Vac. Sci. and Technol. 14 (1977) 17.
[34] E. Sirtl: in Semiconductor Silicon 1977 (Electrochem. Soc., Pennington, N.Y., 1977) p. 4.
[35] A.J.R. De Kock: in Defect in Semicond. (North-Holland Publ. Co., Amsterdam, 1981) 309.
[36] V.V. Voronkov: J. Cryst. Growth 59 (1982) 625.
[37] V. V. Voronkov and M. G. Milvidskii: Kristallografiya, 33 (1988) 471.
[38] V.V. Voronkov and R. Falster: J. Cryst. Growth 194 (1998) 76.
[39] E. Dornberger, W. Von Ammon, J. Virbulis et al. : J. Cryst. Growth 230 (2001) 291.
[40] T.L. Larsen, L. Jensen, A. Lüdge et al. : J. Cryst. Growth 230 (2001) 300.
[41] H. Rauh, D. Sieger and A. Wright: in Defect Control in Semiconductor, vol. 2 (Elsevier, Amsterdam, 1990) p. 1541.
[42] E. Sirtl and A. Adler: Z. Metalkunde 52 (1961) 529.
[43] F. Secco d'Arogona: J. Electrochem. Soc. 119 (1972) 948.
[44] M.F. Ashby and L.M. Brown: Phil. Mag. 8 (1963) 1083.

[45] M.F. Ashby and L.M. Brown: Phil. Mag. 8 (1963) 1649.
[46] M. Rühle: Phys. Stat. Sol. 19 (1967) 279.
[47] J.B. Mitchell and W.L. Bell: Acta Met 24 (1976) 147.
[48] W.L. Bell: J. Appl. Phys. 47 (1976) 1676.
[49] H. Föll and M. Wilkens: Phys. Stat. Sol. (a). 31 (1975) 519.
[50] K. Seigo, K. Masazu, Y. Naotsugu et al.: J. Appl. Phys. 50 (1979) 8240.
[51] S. Kishino, Y. Matsuhita, M. Kanamori and T. Iizuka: Jpn. J. Appl. Phys. 21 (1982) 1.
[52] I.E. Talanin, V.I. Talanin and D.I. Levinson: Materialy electronnoi techniki 4 (2000) 21.
[53] V.I.Talanin, I.E.Talanin and D.I.Levinson: Semic. Sci. and Technol. 17 (2002) 104.
[54] P.B. Hirsh, A. Howie, R.B. Nicholson, et al.: Electron microscopy of thin crystals (Butterworths, London, 1965).
[55] A. Bourret, J. Thibault-Desseaux and D.N. Seidman: J. Appl. Phys. 55 (1984) 825.
[56] M. Rühle, M. Wilkens and N. Essmann: Phys. Stat. Sol. 11 (1965) 819.
[57] M. Rühle: Phys. Stat. Sol. 19 (1967) 263.
[58] M. Wilkens and H. Föll: Phys. Stat. Sol. (a) 49 (1978) 555.
[59] K.H. Katerbau: Phys. Stat. Sol. (a) 38 (1976) 463.
[60] S.M. Ohr: Phys. Stat. Sol. (a) 38 (1976) 553.
[61] M. Wilkens and M. Rühle: Phys. Stat. Sol. (a) 49 (1972) 749.
[62] T.Y. Tan and W.K. Tice: Phil. Mag. 34 (1976) 615.
[63] W.J. Taylor, U. Gösele and T.Y. Tan: J. Appl. Phys. 72 (1992) 2192.
[64] K.N. Neimark, B.A. Sakharov, V.F. Chulitsky and M.I. Osovsky: in Kremnii i Germanii 2 (Metallurgiya, Moscow, 1970) p. 32.
[65] W. Wijaranakula and H.D. Chiou: Appl. Phys. Lett. 64 (1994) 1030.
[66] J.B. Kamm and R. Müller: Sol. State Electr. 20 (1977) 105.
[67] T. Abe, Y. Abe and J. Chikawa: in Semiconductor Silicon 1973 (Princeton, N.Y., Electrochem. Soc., 1973) p. 95.
[68] D.J. Chadi: Phys. Rev. B 41 (1990) 10595.
[69] P. Gall, J.P. Fillard, J. Bonnafe et al.: in Defect Control in Semicond., vol. 1 (Elsevier, Amsterdam, 1990) p. 255.
[70] N.I. Puzanov and A.M. Eidenzon: Semicond. Sci. and Technol. 7 (1992) 406.
[71] A. Ikari, H. Haga, A. Uedono et al. : Jpn. J. Appl. Phys. 33 (1994) 1723.
[72] A. Borghesi, B. Pivac, A. Sassella and A. Stella: J. Appl. Phys. 38 (1995) 4169.
[73] S. Umeno, Y. Yanase, M. Hourai et al. : Jpn. J. Appl. Phys. 38 (1999) 5725.
[74] B.O. Kolbesen and A. Mühbaur: Sol. State Electr. 15 (1982) 759.
[75] F. Shimura, R.S. Hockett and D. A. Reed: Appl. Phys. Lett. 46 (1985) 941.
[76] P.J. Drevinsky, C.E. Caefer, L.C. Kimerling and J. L. Benton: in Defect Control in Semicond., vol. 1 (Elsevier, Amsterdam, 1990) p. 341.
[77] S. Gupta, S. Messoloras, J.R. Schneider et al. : Semicond. Sci. and Technol. 7 (1992) 5.
[78] T. Ueki, M. Itsumi and T. Takeda: Jpn. J. Appl. Phys. 38 (1999) 5695.
[79] V.G. Gorshkov, Yu.K. Danilenko, V.V. Osiko et al. : Phys. Stat. Sol. (a) 106 (1988) 363.
[80] W. Wijaranakula: J. Electrochem. Soc. 139 (1992) 604.
[81] J.L. Lindström and B.G. Svensson: Mat. Res. Soc. Symp. Proc. 59 (1985) 45.
[82] C.A. Londos, N. Sarlis, L.G. Fytros and K. Papasterqiou: Phys. Rev. B 53 (1996). 6900.
[83] N.I. Puzanov and A.M. Eidenzon: Cryst. Rep. 41 (1996) 134.
[84] T.Y. Tan and C.Y. Kung: J. Appl. Phys. 59 (1986) 917.
[85] U. Gösele: Mat. Res. Soc. Symp. Proc. 59 (1986) 419.
[86] F.C. Frank and D. Turnbull: Phys. Rev. 104 (1956) 617.
[87] H. Strunk, U. Gösele and B.O. Kolbesen: Appl. Phys. Lett. 34 (1979) 530.
[88] U. Gösele, W. Frank and A. Seeger: J. Appl. Phys. 23 (1980) 361.
[89] U. Gösele, F.F. Morehead and H. Föll: Semiconductor silicon (Electrochem. Soc., New York, 1981) 766.
[90] N.A. Stolwijk, J. Hölzl, W. Frank et al. : Phys. Stat. Sol. (a) 104 (1987) 225.
[91] H. Kitigawa: Jpn. J. Appl. Phys. 21 (1981) 276
[92] T.Y. Tan, U. Gösele and F.F. Morehead: J. Appl. Phys. 31 (1983) 97.
[93] R.H. Akchurin: in Fizika i materialovedenie poluprovodnikov s glubokimi urovnyami (Metallurgiya, Moscow, 1987) 117.

[94] F.F. Morehead, N.A. Stolwijk, W. Meyberg and U. Gösele: Appl. Phys. Lett. 42 (1983) 690.
[95] T. Okino and M. Onishi: Jpn. J. Appl. Phys. 33 (1994) 6642.
[96] T. Okino, T. Shimosaki and R. Takaue: Jpn. J. Appl. Phys. 36 (1997) 6591.
[97] K. Tempelhoff and N. Van Sung: Phys. Stat. Sol. (a) 72 (1983) 617.
[98] R.B. Fair: J. Appl. Phys. 51 (1980) 5828.
[99] D.A. Antoniadis and I. Moskowitz: J. Appl. Phys. 53 (1982) 6788.
[100] U. Gösele, W. Frank and A. Seeger: Sol. State Commun. 45 (1983) 31.
[101] A. Seeger and K.P. Chik: Phys. Stat. Sol. 29 (1968) 455.
[102] A. Seeger and M. Swanson: in Lattice Defects in Semicond. (Univ. Tokyo Press, Tokyo, 1968) p 93.
[103] A. Seeger: Rad. Eff. 9 (1971) 15.
[104] W. Frank: in Lattice Defects in Semicond. (Wiley, London, 1975) 23.
[105] A. Seeger, H. Föll and W. Frank: in Rad. Eff. in Semicond., Inst. Conf. Ser. N 43 (IOP, Bristol, 1977) p. 12.
[106] A. Seeger, W. Frank and U. Gösele: in Defects and Rad. Eff. in Semicond., Inst. Conf. Ser. N 46 (IOP, Bristol, 1979) p. 148.
[107] J. Dzelme, I. Ertsinsh, B. Zapol and A. Misiuk: Phys. Stat. Sol. (a) 171 (1999) 197.
[108] R. Tognato: Phys. Stat. Sol. (a) 98 (1986) K133.
[109] U. Gösele and T.Y. Tan: in Diffusion in Solids (TransTech Publ., Zürich, 1992) p. 189.
[110] A.L. Aseev, L.I. Fedina, D. Höehl and H. Bartsch: Clusters of interstitial atoms in silicon and germanium (Academie Verlas, Berlin, 1994) 152 p.
[111] P.S. Plekhanov, U. Gösele and T.Y. Tan: J. Appl. Phys. 84 (1998) 718.
[112] L. Fedina, A. Gutakovskii, A. Aseev et al. : Phys. Stat. Sol. (a) 171 (1999) 147.
[113] S. Pizzini: Phys. Stat. Sol. (a) 171 (1999) 123.
[114] T.R. Waite: Phys. Rev. 107 (1957) 463.
[115] L. Fedina, A. Gutakovskii, A. Aseev et. al. : Phil. Mag. A 77 (1998) 423.
[116] M. Ogino: Appl. Phys. Lett. 41 (1983) 847.
[117] R.B. Swaroop: Sol. State Technol. 26 (1983) 111.
[118] F. Shimura, R.S. Hockett, D.A. Reed and D. N. Wayne: Appl. Phys. Lett. 47 (1985) 794.
[119] H. Yamanaka: Jpn. J. Appl. Phys. 33 (1994) 3319.
[120] V.I. Talanin, I.E.Talanin and D.I. Levinson: in Abstr. of ICDC-01 (2001) p. 27.